2011

Surface-enhanced Raman spectroscopy substrates based on nanoporous silicon and pattern transfer

Pallavi Rao Malempati
Louisiana State University and Agricultural and Mechanical College, mrao2@lsu.edu

SURFACE-ENHANCED RAMAN SPECTROSCOPY SUBSTRATES BASED ON NANOPOROUS SILICON AND PATTERN TRANSFER

A Thesis
Submitted to the Graduate Faculty of the
Louisiana State University and
Agricultural and Mechanical College
in partial fulfillment of
the requirements for the degree of
Master of Science in Electrical Engineering
in
The Department of Electrical and Computer Engineering

By
Pallavi Rao Malempati
B.E., Rashtrasant Tukhdoji Maharaj Nagpur University, Nagpur, India, 2006
December 2011

Dedicated to my parents and late brother

Acknowledgements

I am grateful to my major professor, Dr. Dooyoung Hah, for his unending support throughout the course of my thesis. I am indebted to him for encouraging me to explore new ideas and helping me implement them. It was an honor to have Dr. Theda Daniels-Race and Dr. Martin Feldman on my thesis committee. I am grateful to them for being caring and extremely considerate. I acknowledge the support from Highway Safety Research Group for partially funding my Masters' degree.

I would also like to thank Dr. Naga Korivi and Mr. Ragavendra Shankar Murthi for training me on the lab equipment. Mr. Anirban Sarkar made himself available in more ways than one. He guided me through the trivial phases in my research. I sincerely thank Mr. Pradeep Pai, Mr. Karthik Balasubramanian and Ms. Dan Zhang for their technical and non-technical inputs. It was an honor for me to get a chance to work with Dr. Sunggook Park, Mr. Alborz Amirsadeghi, Mr. Bahador Farshchian and Mr. Jiahao Wu.

My parents have been a constant source of unconditional love and support. Their confidence in me encouraged me to pursue a Masters' degree. I can't thank Chris Holbrook enough, for his everlasting support, his faith in my work and me. I owe my deepest gratitude to Harish Kapri for making the toughest situations comforting and for always looking out for me. Ronnie, Jasmine and Stegmutt made the days easy by just being a part of it. Deepali Karwande, Komal Bhagia, Piyush Sharma, Harikrishna Dasari and Abhijeet Verma encouraged me to pursue my dreams and helped me stay focused. I cannot thank them enough for being such a special part of my life. I sincerely thank all my friends and family for all the help and support they provided me with, without which I wouldn't have been able to make this research a success.

Table of Contents

List of Tables

List of Figures

Abstract

Surface-enhanced Raman scattering enhances the weak Raman scattering by using a roughened metal-coated surface as a catalyst. Roughness in the nanometer range provides the best enhancement. The nanostructures for the surface-enhanced Raman spectroscopy (SERS) substrates, in this work, are generated using an electrochemical etching process on silicon substrates. The patterns of nanoporous silicon thus generated are transferred onto transparent polydimethylsiloxane (PDMS) substrates using the "lift-off" process. An incomplex sputtering technique is employed to coat this substrate with a ~20 nm aluminum layer. Rhodamine 6G (R6G) molecules, when adsorbed to this metal surface, form the final SERS substrate that undergoes Raman spectroscopy characterization. This technique is expected to be useful when simple and photolithography-free techniques need to be employed for SERS substrate fabrication.

Chapter 1: Introduction

The conception of a scattered photon, when the electromagnetic radiation hits the molecule under study, actualizes the Raman phenomenon. The annihilation of the incident photon is ensued in the same step. The difference in the energies of these two photons (incident and scattered), helps categorize the phenomenon as either Raman or Rayleigh scattering. If the energies of these two photons are identical, the scattering is called Rayleigh scattering whereas a difference in energies results in Raman scattering (1). Raman scattering of the incident laser forms the backbone of Raman spectroscopy. Since the weak Raman scattering is always accompanied by an aggressive Rayleigh scattering, the results of Raman spectroscopy can be equivocal. Figure 1 explains the Raman and Rayleigh scattering.

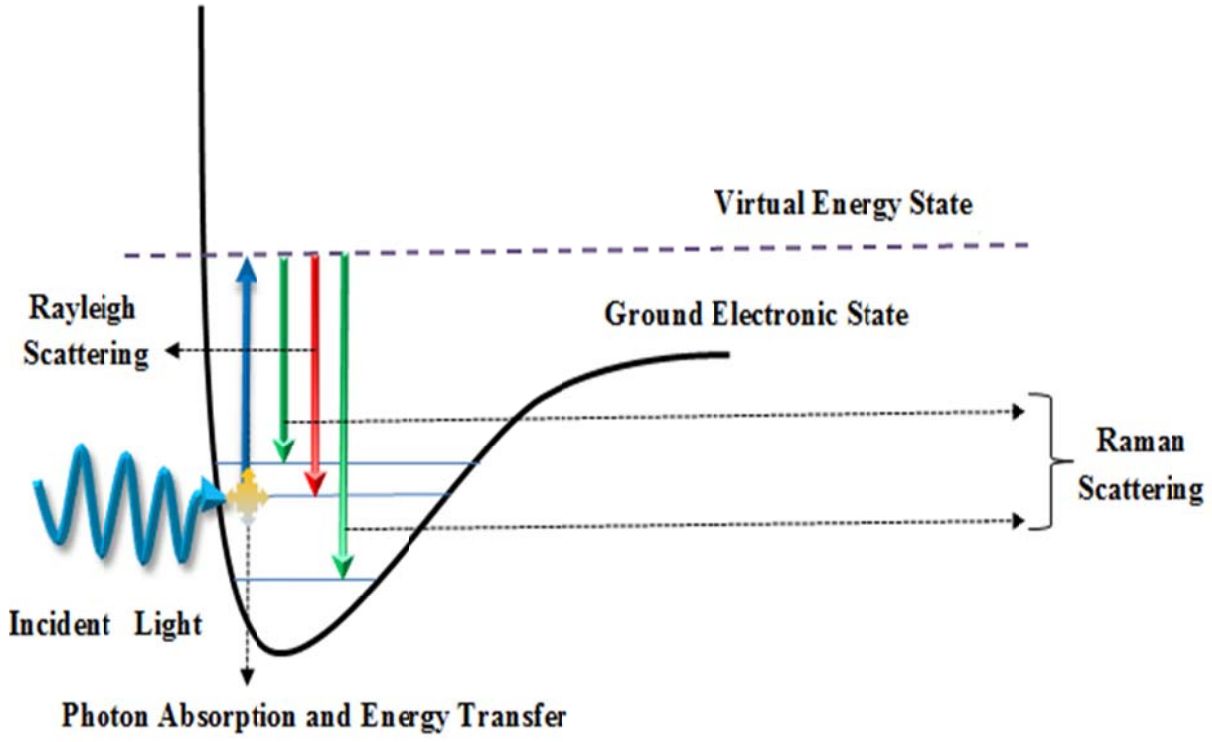

Figure 1: Raman and Rayleigh scattering. Adapted from (2).

1.1 Surface-Enhanced Raman Spectroscopy

The accidental discovery of surface-enhanced Raman scattering (SERS) in 1974 led to major advancements in the field of spectroscopy. The first SERS experiment observed the enhancement of the Raman signal by a magnitude of at least 10^6. This was accomplished by the adsorption of pyridine on the surface of silver nanoparticles (3). At the time, Martin Fleishman explained the large signal from his pyridine experiment to be an after-effect of the large number of scattering molecules present on the surface (4).

A clearer understanding of this signal magnification came in the late 1970's. The most common explanation for this effect is the electromagnetic enhancement effect (5). It accredits the enhancement in the Raman intensity to the electromagnetic field that exists at interfaces, also known as the surface plasmons (6). The incident light breaks ground for the enhancement process, by exciting the surface plasmons. This excitation energy is lost on surfaces that are smooth. When the roughness of the surface is less than the wavelength of the incident radiation, a dipolar plasmon is radiated. If this radiation is in resonance with the Raman or Rayleigh scattering of the molecule, the scatter will be amplified (6).

The other explanation for the enhancement phenomenon is a charge-transfer enhancement effect. This explanation holds true for molecules that bond to the surface. By exciting an electron from the metal surface into an adsorbed molecule, the incident photon creates a negatively charged excited molecule. A nuclear relaxation is induced in the negatively charged excited molecule, as a result of this charge transfer. This relaxation promotes the return of the electron to the metal surface creating an excited neutral molecule. It also results in the emission of a wavelength shifted photon or the Raman photon (6).

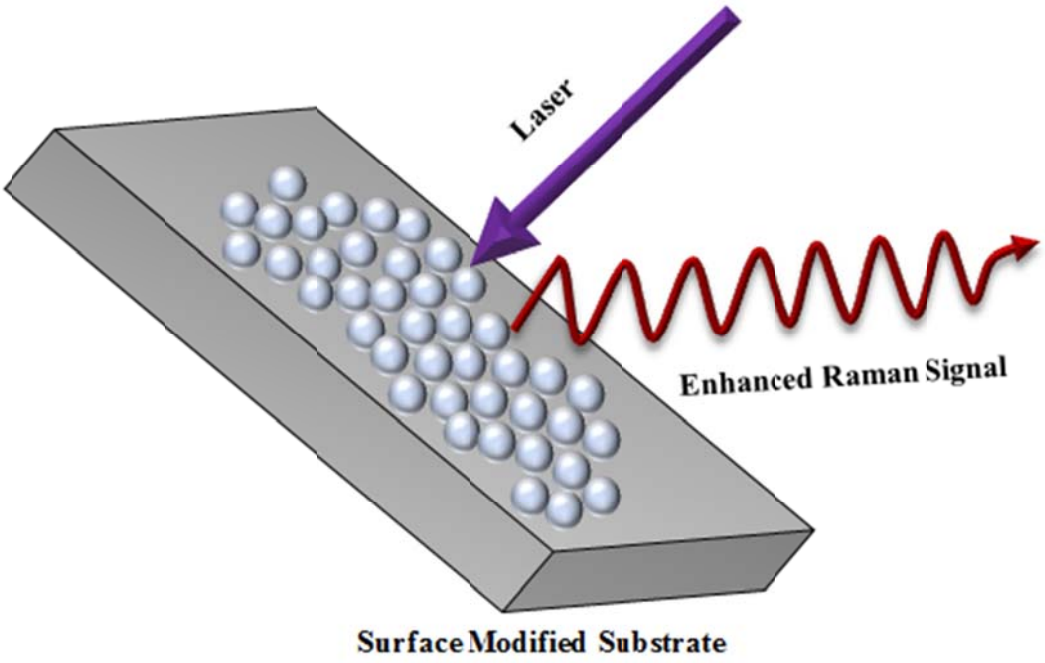

Figure 2: Surface-enhanced Raman spectroscopy. Adapted from (7).

The exact mechanism of the SERS effect is still not completely understood. Figure 2 shows the incident laser and the enhanced Raman signal resulting from a roughened surface.

1.2 Applications of SERS

The high enhancement factor in SERS makes it a very popular technique in not just electrochemistry but also in pharmaceutical industry, geosciences, gemology, forensic science, nanotechnology, art, semiconductors and biosciences (8). Some of the common applications of SERS follow (9).

- Mapping and Imaging (10):

  The distribution of analyte molecules or the hot spots from electromagnetic enhancement can be investigated using point-to-point mapping or global imaging. Point to point mapping can be achieved by raster scanning the substrate and getting the Raman spectra

at desired locations. The data obtained can be used to plot maps and hence examine the various plausible conditions. In global imaging, only frequencies of desired band are allowed to pass through filters. The spatial distribution of the intensity of this band is then captured. Both the methods are used to study the homogeneity and quality of the substrates under study. Since this study is performed at a molecular level, SERS plays a vital role.

- Forensics (11):

  Since SERS is a non-destructive, non-contact, surface sensitive technique, it is a valuable tool in forensics. The process has been used in drug abuse identification and the detection of explosives (11). One fascinating application of SERS, in the fields of biology and forensics, is its use in DNA and RNA detection. A DNA chip containing nucleotide sequences in a grid pattern is used, instead of using only the target DNA. A database holds information about all of these sequences. Since the target DNA combines with the complimentary DNA on the chip alone, the target sequence can be identified. SERS is used to identify the location of this complimentary DNA sequence (12).

- Biomedical Applications (11):

  Bone composition, bone disease state, cancer identification, eye examinations and *in vivo* skin studies currently employ SERS.

1.3 Preparation of the SERS Substrate

Depending on the process used to adsorb the metal on the roughened surface, it can either be colloidal SERS or substrate SERS. The most commonly used metals for SERS substrates are gold, silver and copper.

Colloidal SERS

When metal particles are dispersed in a continuous gas, liquid or solid medium, colloidal SERS is formed (13). The particles remain dispersed in the solution indefinitely. The complexity of the colloid preparation is dependent on the target molecule, the system of analysis of the colloidal substrate and the equipment used for the process. The most commonly employed methods for the preparation of silver and gold colloids are:

- Lee and Meisel Method (14):

  The goal of this method is to study the adsorption of dyes on metal colloids using SERS. This is accomplished by adding trisodium citrate solution to a boiling silver nitrate solution. The dark grey mixture is left boiling for an hour before it is allowed to cool down to form colloidal silver (15).

- Leopold and Lendl Method (16):

  Sodium hydroxide is used to dilute hydroxylamine hydrochloride. This mixture is then rapidly added to a diluted silver nitrate solution. The grey brown colloidal silver is actualized in a few seconds. This method is commonly used when the preparation of colloidal silver needs to be fast and at room temperature (15).

- Creighton Method (17):

  This method is employed when a simple, low cost and time efficient method for preparation of colloidal silver is needed. Aqueous solutions of sodium borohydride and silver nitrate are prepared separately and ice-cooled. The silver nitrate is added drop by drop into the sodium borohydride solution and stirred vigorously. This mixture is then kept still for an hour, before a 10 minute vigorous stirring again. The resulting mixture is colloidal silver (15).

- Sutherland and Winefordner Method (18):

  This technique is employed when a monodisperse layer of colloidal metal is required. Chloroauric acid is added to triply distilled water. Trisodium citrate solution is added drop by drop to the diluted chloroauric acid and then stirred at regular intervals. The mixture is boiled for 5 minutes to get the final dark red colloidal gold (15).

Colloidal suspensions for SERS are not very complex to prepare. The suspensions are also easy to handle and to store. These characteristics contribute towards the popularity of colloidal SERS. But, the high sensitivity to the preparation technique and impurities, limit its performance.

Substrate SERS

Increasing interest in SERS assisted a detailed look into the fabrication techniques for SERS substrates. Some of the work in SERS substrate fabrication employs the following techniques:

- Island Lithography (19) :

  Green *et al.* created a range of pseudo-random silver structures using island lithography and electroless plating. Pyridine was adsorbed onto this substrate. Their study shows that these substrates gave a uniform Raman signal for areas saturated in pyridine and also areas that had less than a monolayer of it. These substrates were robust and reproducible and can be useful in analytical applications.

- Multi-Layer Nanogap Array (20):

  Seol *et al*. fabricated their SERS substrate with a multi-layer nanogap array that consisted of three linearly aligned gold nanogaps. The fabrication process primarily consisted of chemical vapor deposition (CVD) and etching. This technique is used for SERS

substrates when the fabrication steps need to be photolithography-free, simple and reliable. The results confirmed that the enhancement was strongest when the polarization angle was perpendicular to the nanogap. These substrates can be utilized in small-sized electrochemical sensing system.

- Porous Anodic Alumina (PAA) templates (21):

  Li *et al*. fabricated the orderly arranged nanoparticles on a silver film using porous anodic alumina (PAA) templates. A 99.99%-purity silver film, several millimeters thick, was evaporated onto the PAA templates. The SERS substrates were obtained when the PAA templates were removed in hydrochloric acid. The pyridine spectrum that was observed on this sample was 30 times stronger than an Ag film deposited directly on a glass slide.

Sandblasting (22), nanosphere lithography (23), metal island deposition (24) are some of the various approaches that have also been employed for SERS substrate fabrication.

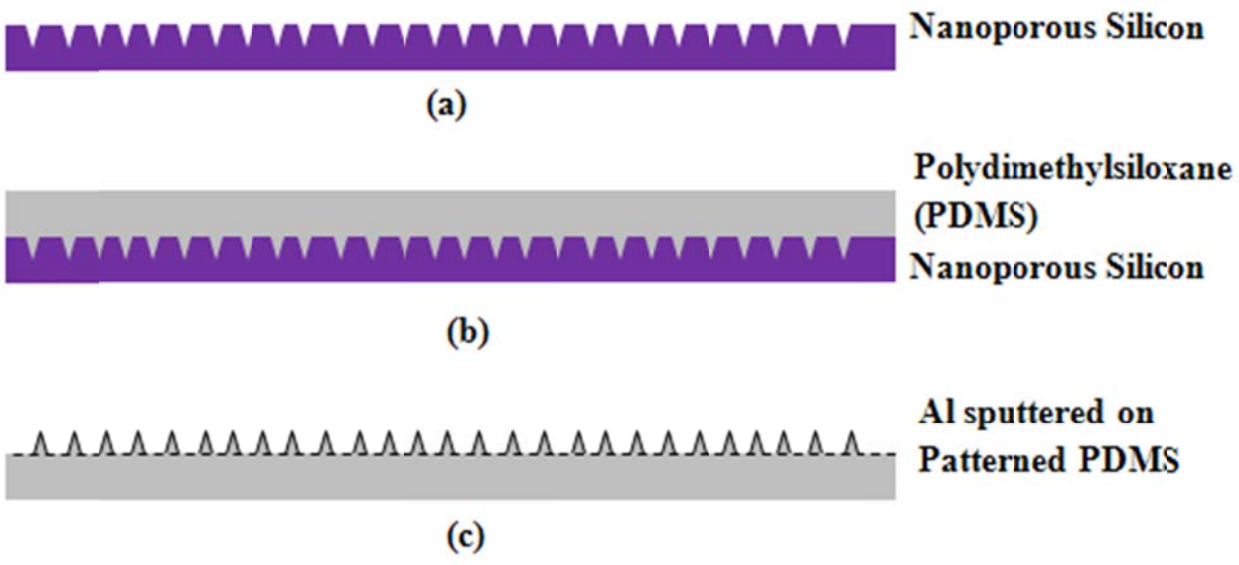

Figure 3: Preparation of the SERS substrate.

In this work, the SERS substrates are prepared using a simpler approach. Figure 3 shows the flow of SERS substrate preparation. It involves three primary steps: the fabrication of nanoporous silicon, pattern transfer onto PDMS and the deposition of metal layer on this roughened PDMS. A brief explanation of all the steps involved, follows:

Nanoporous Silicon

Wet etching technique is used for the fabrication of nanoporous silicon. An aluminum plate is used as the base for the setup. The silicon wafer is placed on top of this Al base. A teflon block, that has a cavity for the HF ethanol mixture, is placed on it. The etching current, the mixing ratio of the etchant and the resistivity of the silicon wafer in use, are the pivotal parameters used for controlling the size and distribution of pores on the wafer. This step is explained in depth in Chapter 2.

Pattern Transfer

PDMS is chosen to be the SERS substrate for two primary reasons. First, it can be a very flexible substrate. Second, it is transparent for wavelengths typically used in SERS and hence readings can be taken from the back side of the surface.

Nanoporous silicon pattern is transferred onto the PDMS substrate in order to generate surface roughness. 10 parts of PDMS prepolymer and 1 part of curing agent are mixed and then poured onto the silicon surface. This PDMS is allowed to cure at room temperature for 24 hours before "lift-off".

Sputtering

Sputtering is used to deposit a thin layer of aluminum on the roughened surface. Aluminum has

good adhesion to PDMS and has been known to bring out high SERS enhancement. Two things need to be taken into consideration when determining the thickness of the metal layer to be deposited – smoothening of the surface after deposition and the light absorption for backside illumination. It was reported that SERS signal was six times weaker with the backside illumination compared to the front side illumination for a 75 nm thick silver film (25).

1.3.1 Literature Review

- **Nanoporous Silicon**

The high cost and specializations required for using conventional techniques like electron-beam lithography for the skeleton substrate fabrication gives porous silicon an edge. The fabrication is relatively easy. The shape and size can be easily controlled with slight modifications to the preparation process. Panarin *et al.* used a homogenous porous silicon layer for the fabrication of SERS substrates. The porous silicon obtained on a low resistivity (100) wafer was coated with silver using immersion plating. It was concluded that the microstructure of the silver film and hence the SERS-activity, were dependent on the pore diameter, the porosity and the depth of the pores forming this layer (26). Chan *et al.* compared their SERS-active porous gold substrate against a commercial SERS active substrate namely Klarite®. The gold was deposited on the porous silicon structure using sputtering. It was observed that the molecules adsorbed on the gold/porous silicon substrate had higher sensitivity as compared to Klarite® (27). There are numerous other studies that indicate the effectiveness of porous silicon as a SERS substrate.

- **PDMS**

The high flexibility and the transparency of PDMS make it a very good candidate for SERS substrates. Nahla A. Abu-Hatab, when researching the novel approaches in the fabrication of

SERS substrates, transferred metallic nanodiscs onto PDMS. This structure was used in multiplexed microfluidics platform to produce efficient SERS substrates (28). Wu *et al.* fabricated metallic nanocrack based SERS substrate on PDMS (29). An uneven strain distribution was applied across this substrate to obtain nanocracks. The PDMS used for this purpose was mixed in a 10:1 ratio, where the PDMS prepolymer was 10 parts and the curing agent 1. The results obtained showed an enhancement factor of 4×10^6.

1.4 Challenges

The morphology of nanoporous silicon is controlled by several factors including the wafer resistivity, the etching current and the mixing ratio of the etching solution. The wafer resistivity is not uniform throughout the wafer resulting in non-uniform pore size and depth. To ensure as uniform a current distribution as possible, the silicon wafer will be coated with a 500 nm layer of aluminum on the backside.

In order to transfer the patterns of nanostructures from nanoporous silicon to PDMS, a mixture consisting of 7 parts of PDMS prepolymer and 1 part curing agent was poured onto the nanoporous silicon sample. Since the resulting PDMS was inflexible, it was difficult to "lift-off" without damaging the samples. A mold release agent, 1H,1H,2H,2H-perfluorodecyltrichlorosilane (silane), was tested to help assist the "lift-off". Even though it proved to be an excellent choice for the process, other options were explored. Silane has high toxicity and requires cautious handling. A softer PDMS (10 parts to 1) demonstrated results comparable to samples generated using the silane catalyst. To ensure that the pattern is transferred successfully to soft PDMS, the pores will be formed shallow. Deep pores led to complications in the "lift-off" process. For more flexible PDMS, structures in the micrometer range tend to collapse, jeopardizing the integrity of the entire substrate.

Chapter 2: SERS Substrates

In 1956, Uhlir discovered porous silicon when experimenting with a technique to polish the surface of silicon (30). Instead of an electropolished wafer, an amalgamation of the applied current and the etching solution led to the formation of porous silicon on the wafer. The availability of large surface area on porous silicon generated a lot of interest. The discovery of its room temperature photoluminescence properties in 1990 (31) made porous silicon marketable. Good thermal insulation capabilities and mechanical properties combined with the photoluminescence properties make porous silicon an attractive choice in the silicon industry. The low cost and compatibility with silicon-based electronics are added advantages (32).

2.1 Porous Silicon

Porous silicon is formed by selective etching of silicon substrate. In the early history of porous silicon research, it was assumed to be a layer deposited on the silicon as a result of reduction of divalent silicon to amorphous silicon (33). Years after its discovery came a detailed explanation of pore formation that contradicted this reduction theory.

An externally applied potential to the porous silicon fabrication cell triggers the flow of current from silicon to the HF ethanol mixture. Holes from the semiconductor and F^- ions from the electrolyte combine at the silicon/electrolyte interface to dissolve silicon by process of an electrochemical reaction. A depletion zone starts at this interface. Since anodization is typically maximum at pore tips, the depletion width is limited. The current pinches off when the adjoining depletion layers come in contact. A sudden current pinch curbs further etching. This is very critical in preventing pore structures from collapsing. It is this very self-limiting nature of the process that leads to the formation of porous silicon. When the depletion layers stop widening, deepening of the pores initializes. Formation of the porous silicon layer marks the end of the

electrochemical etching process (32). If applied current is high, the silicon wafer will be electropolished (32).

Pore formation starts at the defects and continues layer by layer (34). To successfully accomplish pore formation, holes need to be the primary carriers of current. N-type and p-type wafers can both be considered for the fabrication of porous silicon. Since the primary carriers in n-type wafers are electrons, external illumination is required to generate enough holes for the pore formation process.

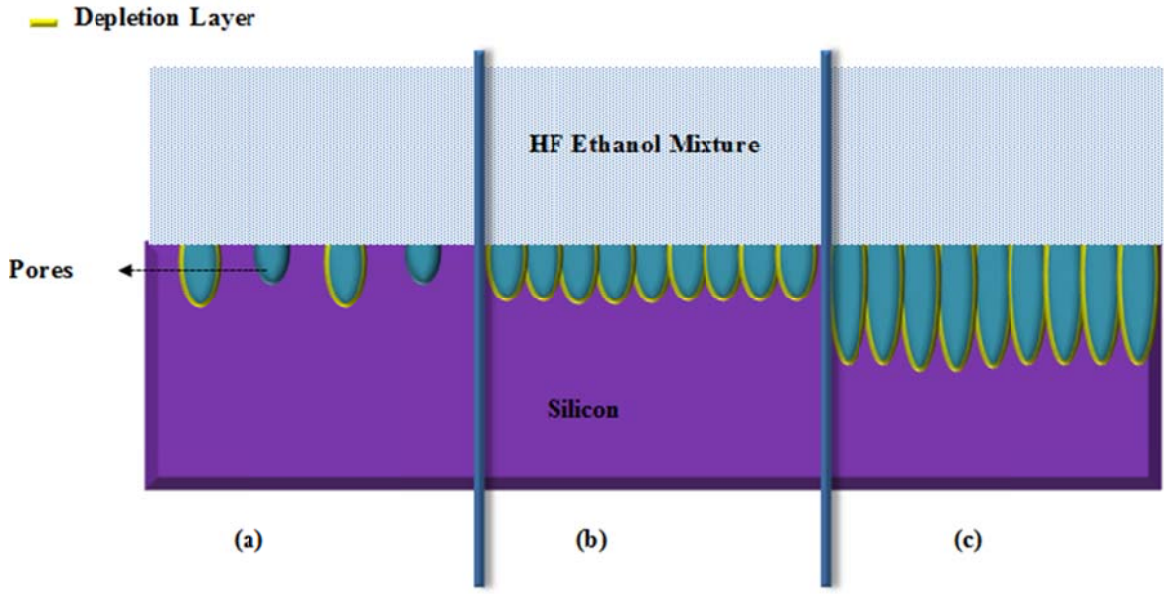

Figure 4: Pore formation in silicon wafer. (a) Formation of depletion layer at silicon/electrolyte interface. (b) Increase in pore depth and width until the depletion layers of adjacent pores touch each other. (c) Increase in pore depth as a result of the current pinching off.

Figure 4 explains the pore formation in brief. Figure 4(a) shows the formation of the depletion layer at the silicon-electrolyte interface (32). Figure 4(b) indicates the increase in the depth of the pores. This is understood to be the result of the sudden pinching off of the current where the

neighboring depletion layers meet, preventing further etching (32). At this point, the holes are present at the tip of the pores and hence the only etching that occurs (32), occurs along this direction, as shown in figure 4(c). Thus, the depth and the porosity of the sample can be controlled by current density, the mixing ratio of the etching solution and the doping concentration of the silicon wafer in use.

Source of the holes defines the direction of pore growth. The alignment of pores is usually decided by roughness of pore walls. The pores are usually aligned along <100> direction.

The morphology of the porous silicon is understood to be primarily dependent on the following parameters:

- Doping concentration (35):

  The effects of a change in doping concentrations are different for p-type and n-type silicon wafers. For n-type silicon, with an increase in doping, the pore size decreases. However, for p-type silicon, size of the pores increases with an increase in doping concentration. It is also observed that two-layered porous silicon can be generated on lightly-doped p-type silicon and illuminated n-type silicon.

- Current density (35):

  When the current density is high, disintegration of silicon and oxide formation occurs. But for lower current densities, only the disintegration of silicon takes place. When the applied current is such that it assists in oxide formation of pore tips, an increase in the current density aids the widening of the oxide layer at the pore bottom alone. The pores thus formed have wider bottoms and thinner walls. However, if the current density is less than that required for the oxide layer formation, an increase in current density increases the current flow through the tip of the pore resulting in sharper pores.

- Mixing ratio of the etching solution (35):

  The mixing ratio of the etching solution, the current density and the doping concentration are inter-related. For effect of the change in mixing ratio to be noticeable, the applied current should be equal to or greater than the value that marks the onset of oxide layer formation at pore tips. If the HF concentration is increased at this point, rate of disintegration of oxide increases. The current density at which the surface is covered with oxide is now higher than with a lower concentration of HF. Smaller pores are an offshoot of this process.

In one study, gold nanocrystals ~63 nm in width were considered to form highly efficient SERS substrates (36). In another research, a very detailed study was done on size dependent enhancement. It was observed that the enhancement was most efficient in the 50 – 200 nm range (37). This work aims at generating pores in this range. The pore morphology is a vital part of this research and hence considerable attention was paid to all of these mutually related parameters.

2.2 Fabrication of Porous Silicon

Two of the most common techniques used for the fabrication of porous silicon are – stain etching and electrochemical etching of the silicon wafer. Stain Etching is often referred to as open-circuit stain etch. A mixture of hydrofluoric acid, nitric acid and water is used as the etchant, usually with a ratio of 1:5:10. The easy availability of the chemicals involved and the ease of fabrication make this process promising. However, its limited usability stems from the fact that the porous silicon layer thus emanated is usually very thin.

Electrochemical etching is a more recurrently used technique for the fabrication of porous silicon. Figure 5 shows the anodization cell used in this research.

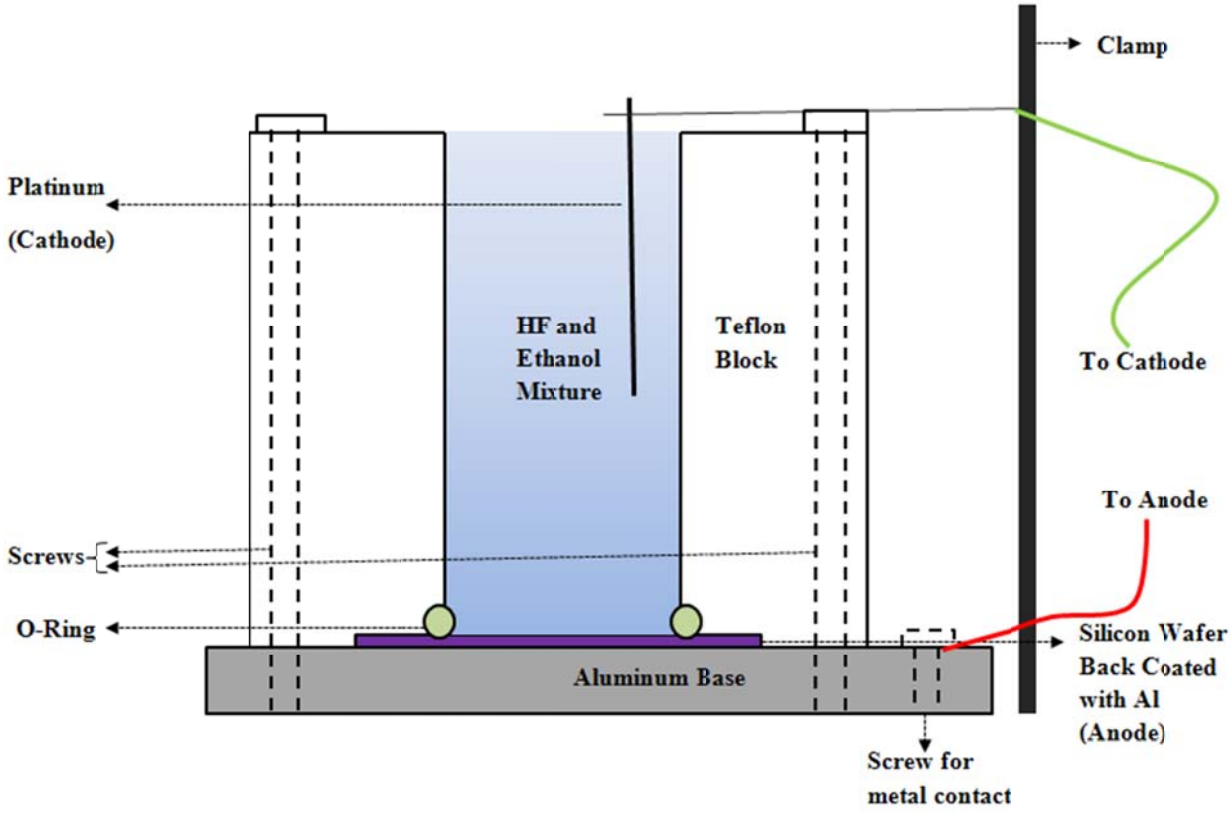

Figure 5: Setup for the fabrication of porous silicon. Figure not to scale.

The 5”×5”×0.5” aluminum plate forms the base for the setup. Aluminum is used as the base to allow electrical connectivity to the current source. A 3” (O.D.) teflon block with a 1” inner diameter is used to hold up to 15 ml of the HF and ethanol mixture. 8 holes are drilled into this block to ensure equal pressure distribution when the screws are tightened to fix the teflon block in place. An O-ring is used to ensure that the HF and ethanol mixture is sealed in. It also eases the stress on the silicon wafer when the teflon block is placed on it. The back side of this wafer is coated with aluminum to ensure uniform distribution of voltage across the silicon wafer. A clamp is used to help dip the cathode (platinum wire) into the etchant.

High resistivity silicon wafers command a lot of attention from the CMOS industry - the primary reason for this being the uniform and stable resistivity throughout the wafer (38). These two factors also contribute towards the formation of a homogenous porous silicon layer. Silicon

wafers with high (1–100 ohm-cm) and low resistivity (0.01-0.02 ohm-cm) were both studied for this research. First tests for the generation of porous silicon were done on high resistivity wafers. HF and ethanol were mixed in a 1:1 ratio. Figure 6 shows all the time and current combinations used on the high resistivity wafer with the HF/ethanol ratio of 1:1.

An average current density of 6 mA/cm^2 showed very little signs of etching for durations of 10, 20 and 30 minutes. However, treated for 60 minutes at 6 mA/cm^2, pores 5-7 μm in diameter were formed. An applied density of 12 mA/cm^2 for 10 minutes showed no etching.

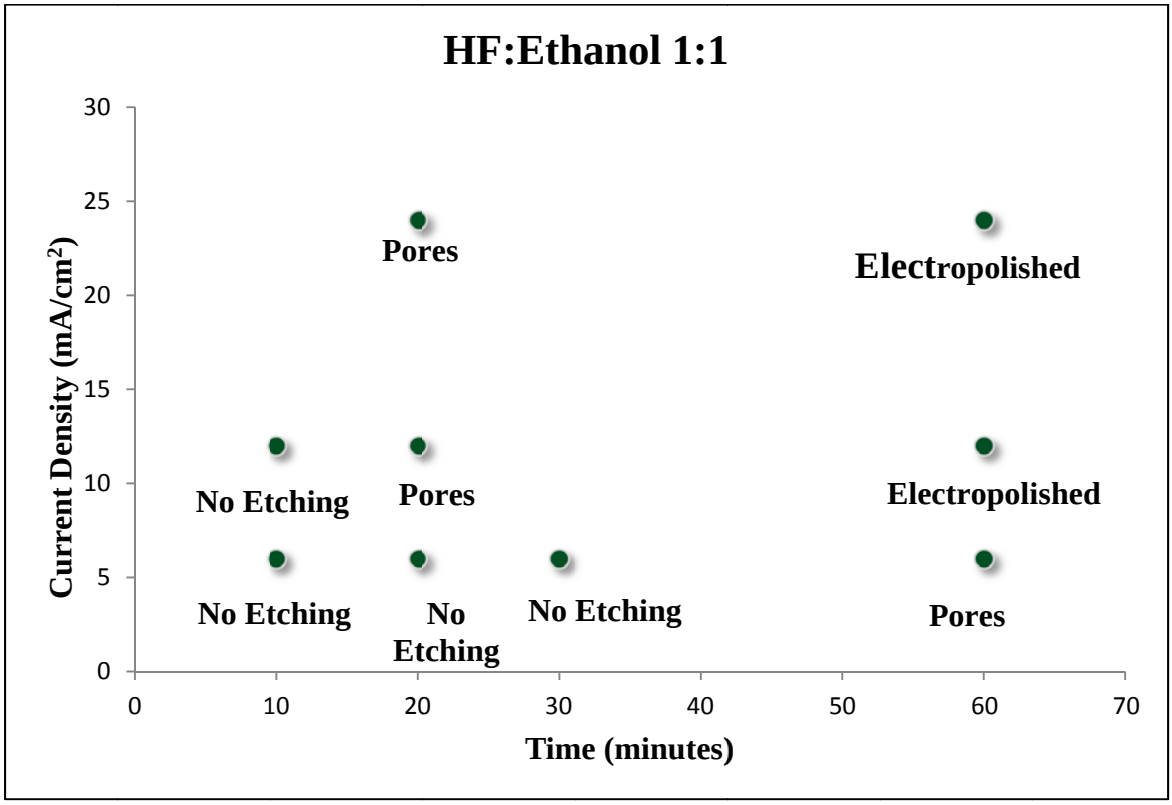

Figure 6: Current v/s time conditions used for high resistivity silicon wafer for the HF/ethanol ratio of 1:1.

Nevertheless, pores 5-7 μm were observed when the sample was etched for 20 minutes at the same current level. The samples that were treated with the etchant for 60 minutes at 12 mA/cm^2 and 24 mA/cm^2 were both electropolished. However, the sample that was etched at 24 mA/cm^2

for 20 minutes generated pores in the μm range. Since the generation of porous silicon was so sensitive to applied current and the etching time on high resistivity wafers, low resistivity wafers were tested. Table 1 shows the time/current combinations that the samples were subjected to.

Table 1: Conditions under which low resistivity samples are treated.

HF: Ethanol 1:1

Current Density (mA/cm^2)	**Etching Time (Minutes)**
6	20
12	20
24	20
24	60
72	20
72	40
90	20
90	25
100	20
100	25
110	20
110	35
120	20
126	20
126	10

The best results with the low resistivity wafers were obtained when the applied current was between 90 mA/cm^2 and 126 mA/cm^2 and the etching time was 20 minutes. A 1-to-1 ratio of HF and ethanol worked best (for the purposes of this work) with the aforementioned conditions. Lower concentrations of HF were also tested but yielded no useful results for the purposes of this work.

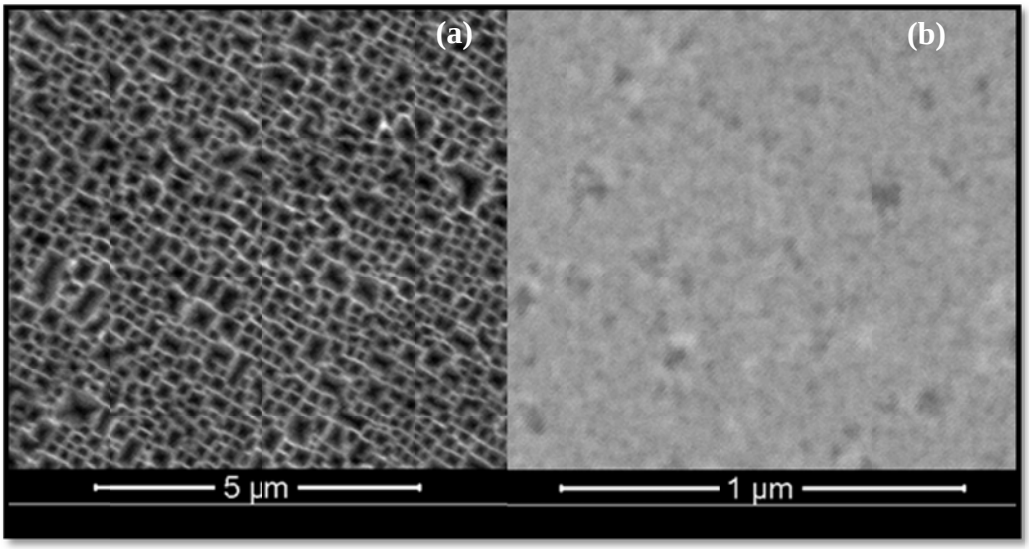

Figure 7: Scanning electron microscopy (SEM) images of porous silicon produced with an applied current density of 120 mA/cm^2. The current was applied for 20 minutes with an HF: ethanol ratio of 1:1. (a) High porosity porous structure at the center of the substrate. (b) Low porosity porous structure on the edge of the substrate.

The pore size was measured to be approximately 50 – 100nm. Figure 7 shows the scanning electron microscopy (SEM) images of different regions on the sample generated at 120 mA/cm^2.

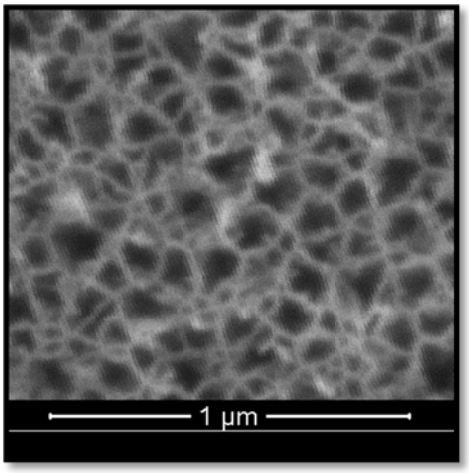

Figure 8 : Porous structure for sample treated for 35 minutes with an applied current of 90mA/cm^2 and HF: ethanol of 1:1.

Figure 8 shows the porous structure that is observed for a sample that is generated when a current density of 90 mA/cm^2 is applied for 20 minutes, with an HF: ethanol of 1:1. Figure 9

shows SEM image of the sample that had a ~ 20 nm Al layer deposited on nanostructures generated at 120 mA/cm^2.

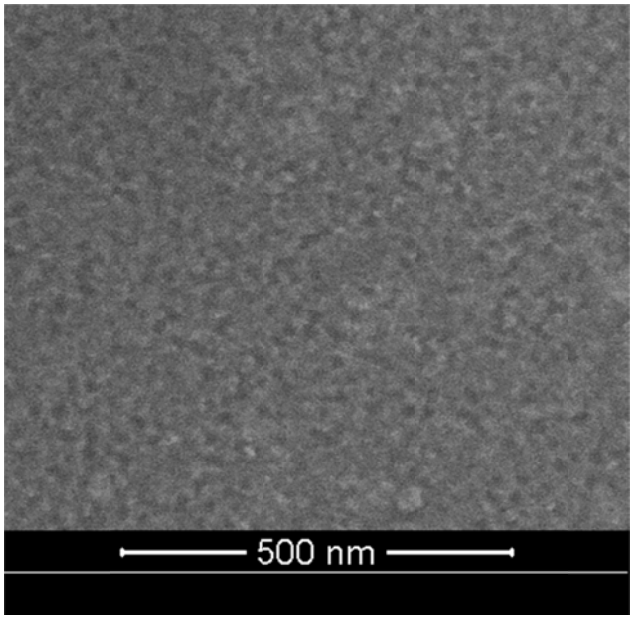

Figure 9: SEM image of metal deposited on nanoporous silicon generated at 120 mA/cm^2.

2.3 PDMS for Pattern Transfer

The high flexibility and transparency of PDMS make it a suitable candidate for SERS substrates useable in the backside illumination arrangement. The PDMS samples used for this work were tested with PDMS prepolymer and the curing agent ratios of 10:1 and 7:1. Patterns were transferred from the silicon substrate onto PDMS using the "lift-off" process. 7-to-1 mixture was poured onto the nanoporous silicon and cured at 80oC for 8 hours. Tearing of the PDMS was observed in high porosity areas during "lift-off". 10-to-1 mixture, cured for a day at room temperature, was then tested on the nanoporous silicon samples. The peeling required extreme caution but the tearing was minimal. To further reduce the tearing, some test samples were coated with a mold release agent - 1H,1H,2H,2H-perfluorodecyltrichlorosilane (silane). The "lift-off" process was effortless and there was practically no damage to the PDMS sample. The

high toxicity of silane and the extreme caution for handling it, restricted its use in this work. The PDMS samples used in this research are shown in figure 10. As a consequence of the minute porous structure, figure 10(b) does not show the roughened PDMS distinctly. The pattern was transferred onto this PDMS from a sample that was treated for 20 minutes, at a current density of 90 mA/cm2 and an HF: ethanol ratio of 1:1.

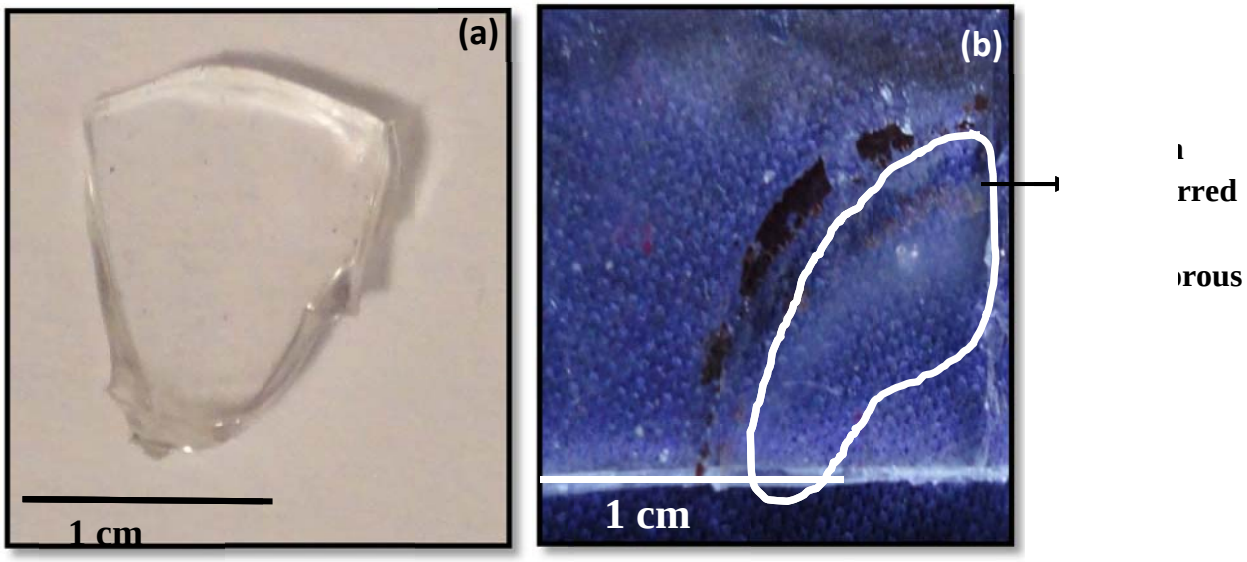

Figure 10: (a) Smooth PDMS. (b) Pattern transferred onto PDMS.

2.4 SERS Substrates

R6G is one of the most popular analytes in Raman spectroscopy. This research uses R6G in the same context. In order to coat the samples with it, they were left in an aqueous solution of R6G for 30 minutes. The samples were then nitrogen dried and placed in a desiccator until. Figures 11– 14 show all the substrates used in this work. Samples shown in Figure 11 were generated when a current density of 120 mA/cm^2 was applied for 20 minutes. The HF: ethanol ratio was 1:1. Figure 11(b) shows sample that has a ~15-20 nm aluminum layer sputtered onto it. Both the samples were dipped in an aqueous R6G for 30 minutes. The samples were then nitrogen dried.

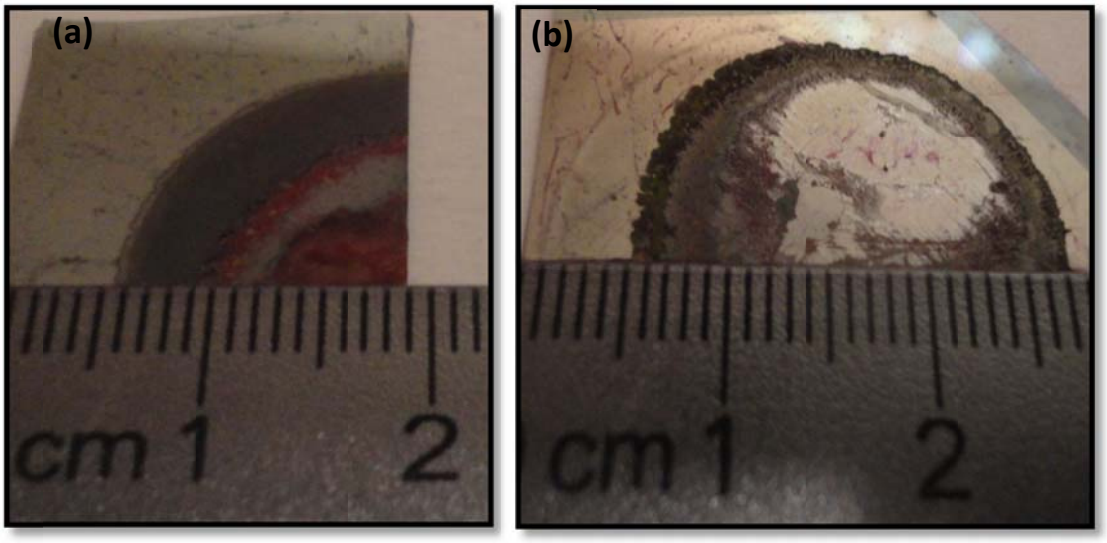

Figure 11: R6G-coated porous silicon substrates. Applied current density: 120 mA/cm^2 etching time 20 minutes ethanol: HF 1:1. Samples are dipped in aqueous R6G for 30 minutes. (a) No metal coating. (b) With ~15-20 nm aluminum coating.

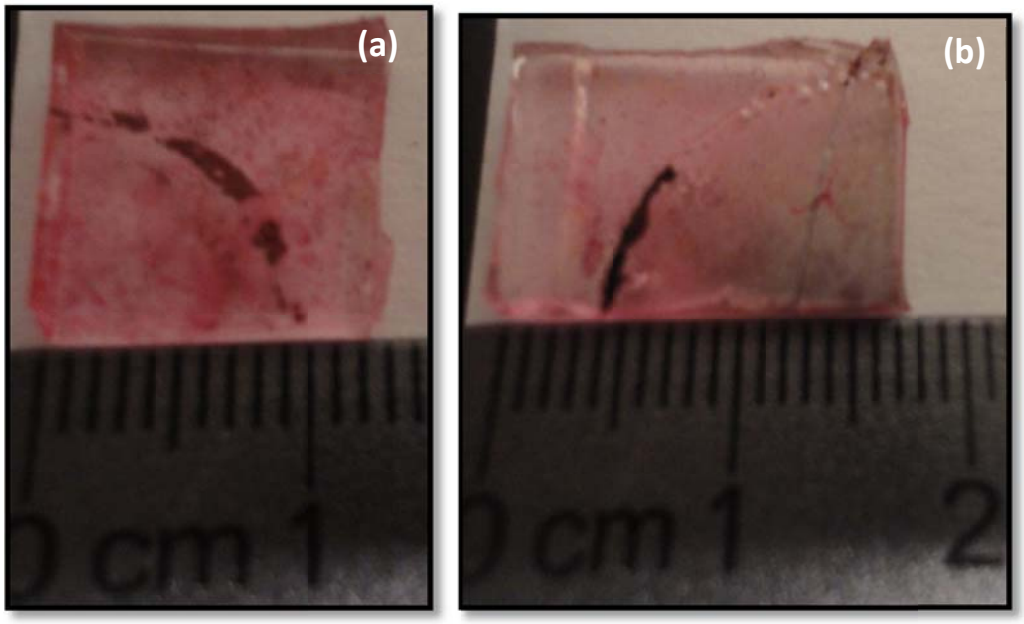

Figure 12 R6G-coated, nanostructure-pattern-transferred PDMS substrates. Applied current density : 90 mA/cm^2, etching time 20 minutes, HF:ethanol 1:1. (a) No metal coating. (b) With a 15-20 nm layer of aluminum.

The structures on the samples in figure 12(a) and (b) were generated when a current density of 120 mA/cm^2 was applied for 20 minutes. The HF:ethanol ratio, for the pore structure formation,

was 1:1. The pattern was transferred from the silicon wafer to the PDMS sample using the "lift-off" process. A 15-20 nm (approximately) aluminum layer was sputtered onto the sample shown in figure 12(b). Both these samples were then dipped into aqueous R6G for 30 minutes and nitrogen dried to stay consistent with the samples shown in figure 11.

The PDMS in figure 13 was prepared by mixing 10 parts of PDMS prepolymer to 1 part of curing agent. The PDMS was cured at room temperature for a day. The samples were then dipped into aqueous R6G for 30 minutes and nitrogen dried. Figure 13 shows a silicon sample dipped in R6G for 30 minutes.

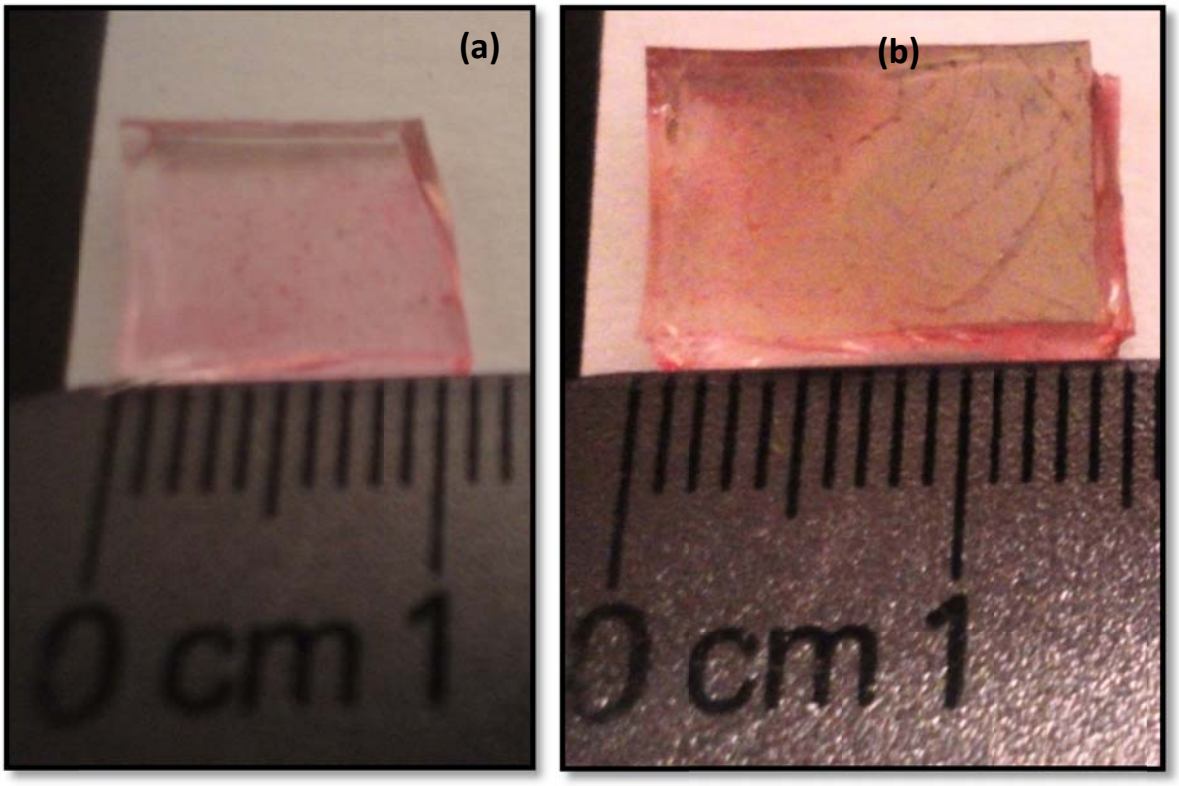

Figure 13 Smooth PDMS substrates. PDMS prepolymer:curing agent 10:1, dipped in R6G for 30 minutes and nitrogen dried. (a) No metal coating. (b) With a 15-20nm layer of aluminum.

Figure 14 shows the smooth silicon sample that was dipped in R6G for 30 minutes and then nitrogen dried.

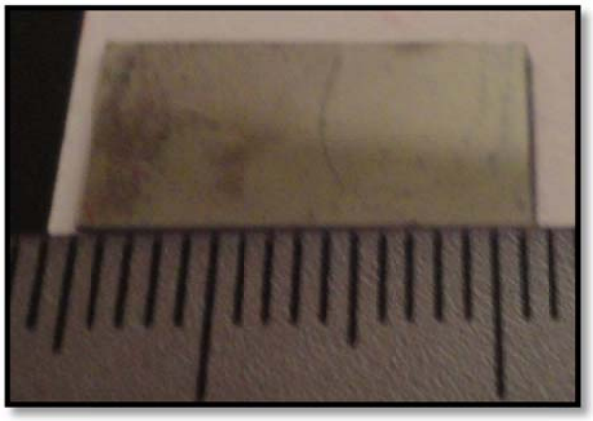

Figure 14: Silicon sample without pores, dipped in R6G for 30 minutes.

Chapter 3: Raman Spectroscopy

An excitation laser, a sample illumination system and light collection optics, a wavelength selector and a detector are the rudimentary components of a Raman system (39). The illumination of the sample is usually done using a visible range laser (39). In our case, the laser is a He-Ne laser with a wavelength of ~633 nm. When the laser beam strikes the sample, there will be some scattering. Most of this scattered signal is collected with the lens. The Raman spectrum is achieved after this scattered light is sent through the interference filter or the spectrophotometer (39). Like discussed in Chapter 1, the results of Raman spectroscopy are extremely useful in the wide range of industries. It is also an excellent tool for research.

Porosity of the porous layer plays a part in the enhancement effect. For structures that have low porosity, the pores are widely spaced and are expected to be stronger. Whereas, high porosity samples have pores separated by thin walls. The “lift-off" process can damage these thin walls. Low porosity samples are thus expected to be suitable candidates for the SERS characterisation.

In this research, the Horiba LabRAM Raman spectrometer is used to study the samples. The samples were studied with a 10× objective lens. Using a 10× instead of a 50× or a 100× objective lens would increase the spot size of the area under study. Whitney *et al*., in their detailed work explained the contribution of the spot size in the Raman spectra. It was concluded that with increasing spot size, the details in the Raman spectra are lost (40). According to their research, the peaks, when a 100× objective is used, indicate a clear contrast whereas as the peaks at 10× give very litte information about the Raman peaks. Since the samples were very close to the 50× and the 100× and ran the risk of being damamged by the sample, when focused, the 10× objective lens was used.

3.1 Reference Samples

This research studies a wide variety of substrates for its Raman behavior. The Raman spectrum for smooth PDMS, without R6G molecules adsorbed on it, is shown in figure 15. The most prominent peaks for the smooth PDMS were observed at 618, 714, 1260 and 1411 cm^{-1}. These peaks are close to the peaks observed by Bae *et al*. in their work (41).

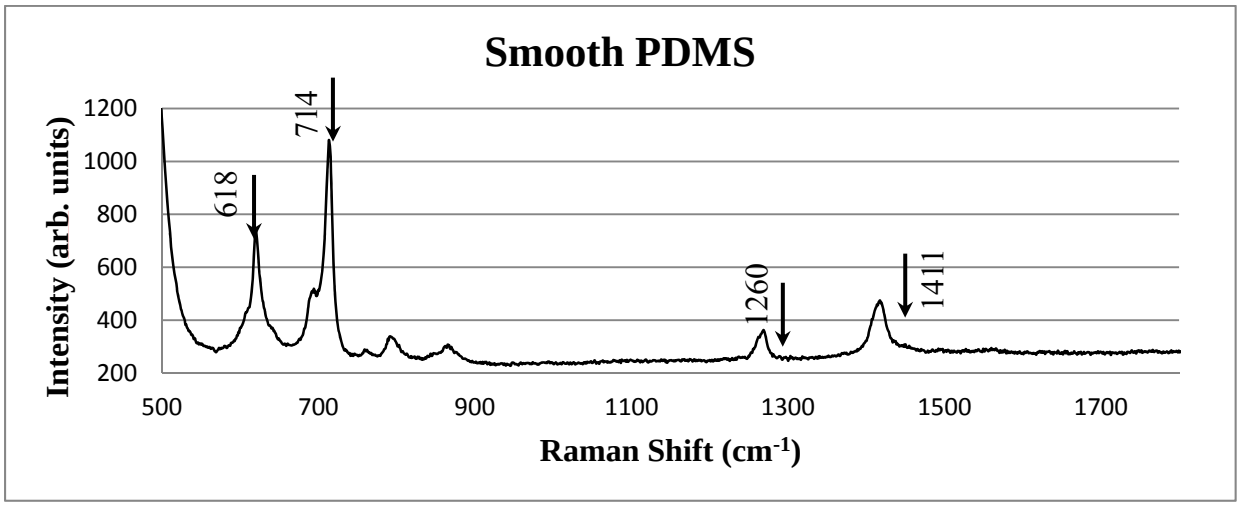

Figure 15: Raman Spectra for Smooth PDMS without R6G

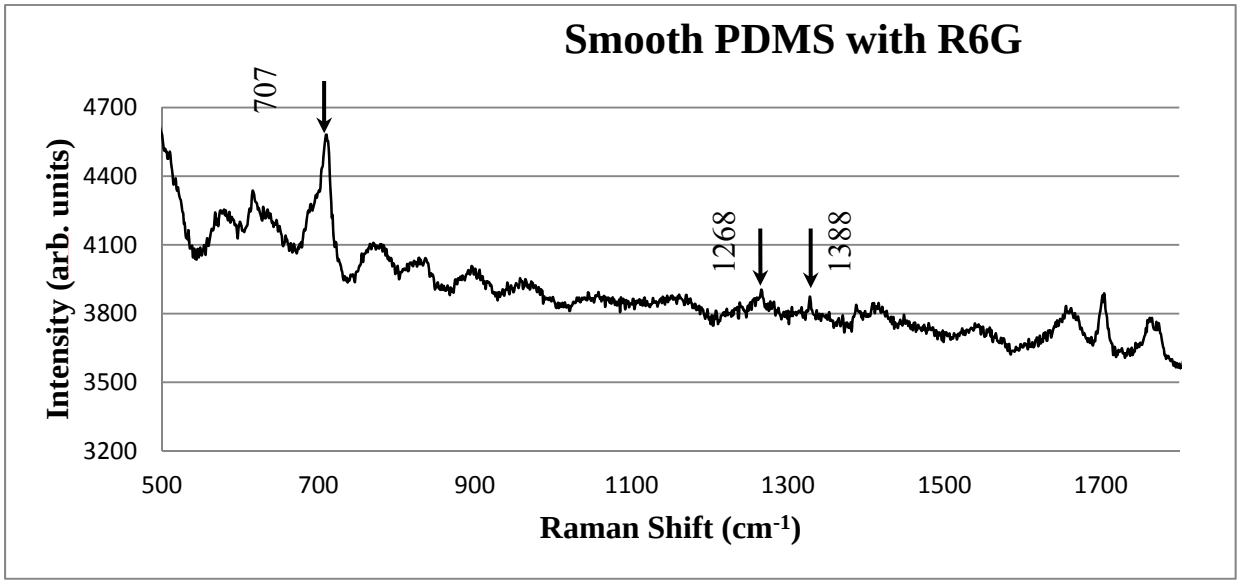

Figure 16: Raman spectra for smooth PDMS with R6G molecules adsorbed on the surface.

Figure 16 shows these Raman spectra peaks on a smooth PDMS sample coated with R6G. The R6G peaks shown, are at 710, 1263 and 1388 cm^{-1}. The peaks at 710 cm^{-1} and 1263 cm^{-1} are consistent with the peaks observed for R6G by Bae *et al* (41). The peak at 1388 cm^{-1} is also a peak for R6G (42).

Figure 17 shows the Raman spectra for a smooth PDMS with an Al layer. The laser was incident on this sample from the front.

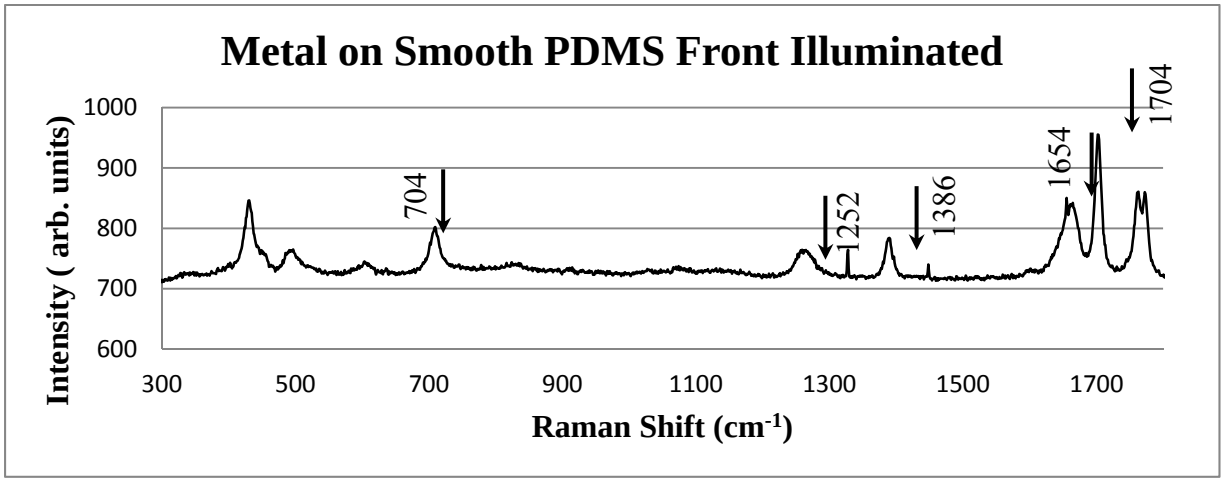

Figure 17 : Raman spectra for smooth PDMS coated with Al and R6G, front illuminated.

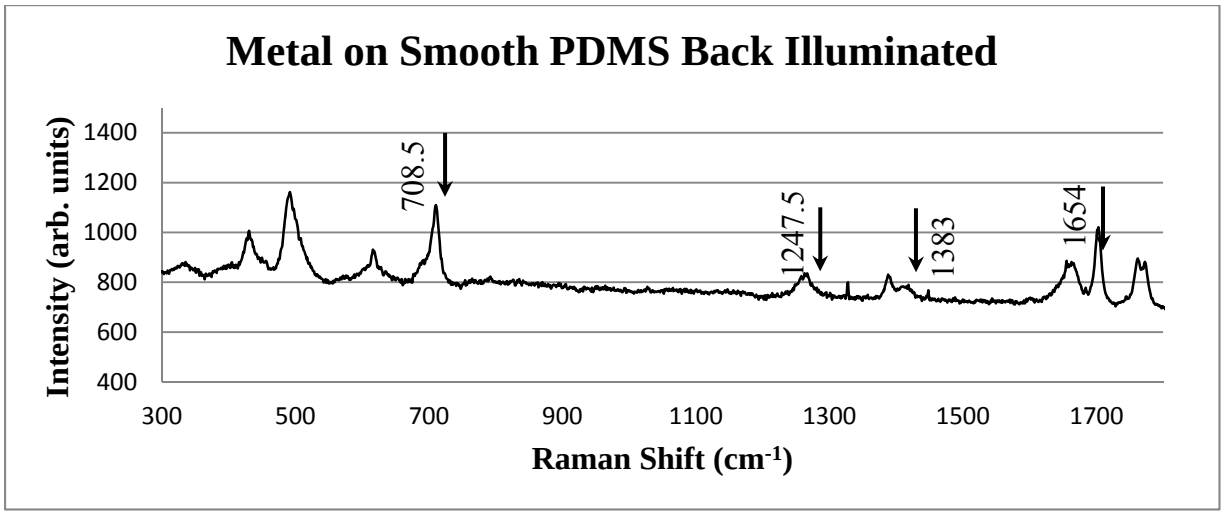

Figure 18: Raman Spectra for smooth PDMS coated with Al and R6G, back illuminated.

Figure 18 shows the Raman spectra for a smooth PDMS sample coated with metal and R6G, when back illuminated. Figure 19 shows the Raman spectra for smooth silicon dipped in R6G.

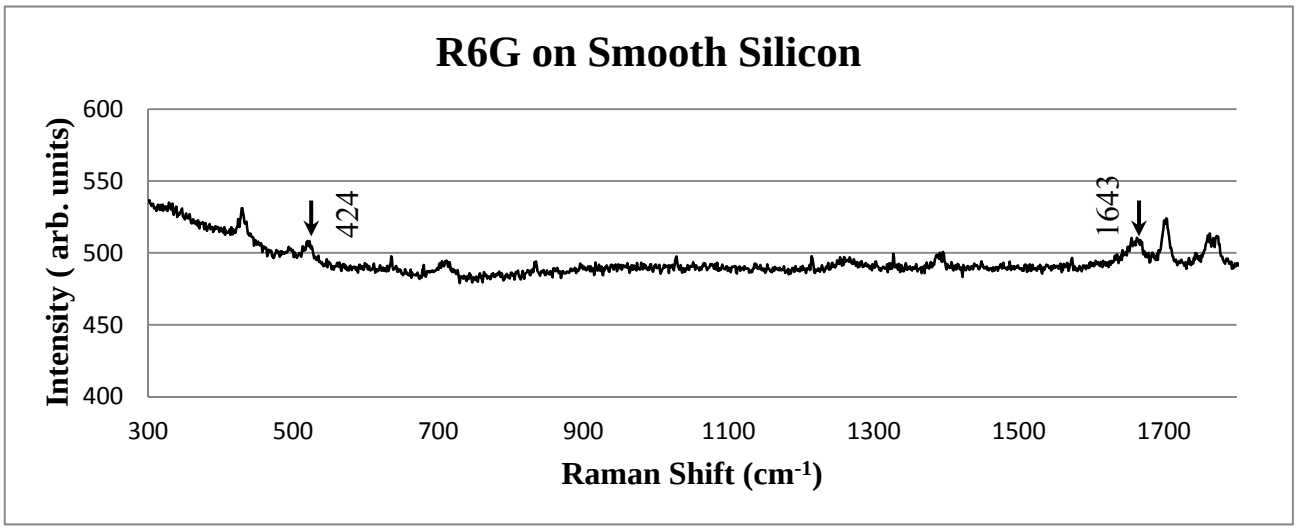

Figure 19 : Raman spectra for smooth silicon dipped in R6G.

For all the reference samples, it was observed that the spot size was small and the peaks sharp.

3.2 Raman Spectra for 90 mA/cm^2 Reference Samples

Pattern was transferred from a 90 mA/cm^2 porous silicon sample to PDMS to generate Raman spectra of Figures 20 and 21. Figure 20 shows the front illuminated sample for this spectrum.

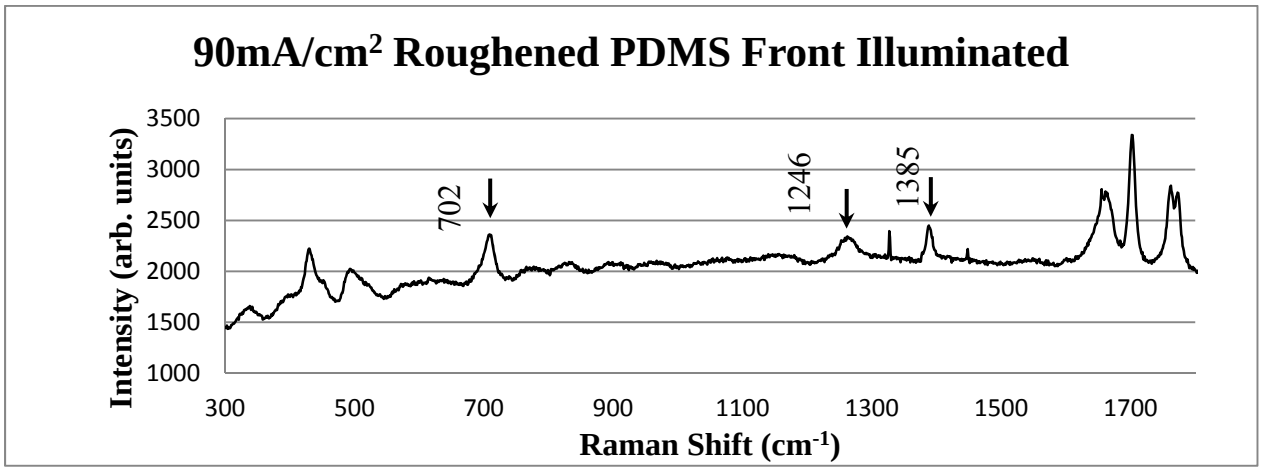

Figure 20 : Front illuminated 90mA/cm^2 porous silicon pattern transferred onto PDMS, dipped in R6G.

Figure 21 shows the Raman spectra for the sample, when back illuminated.

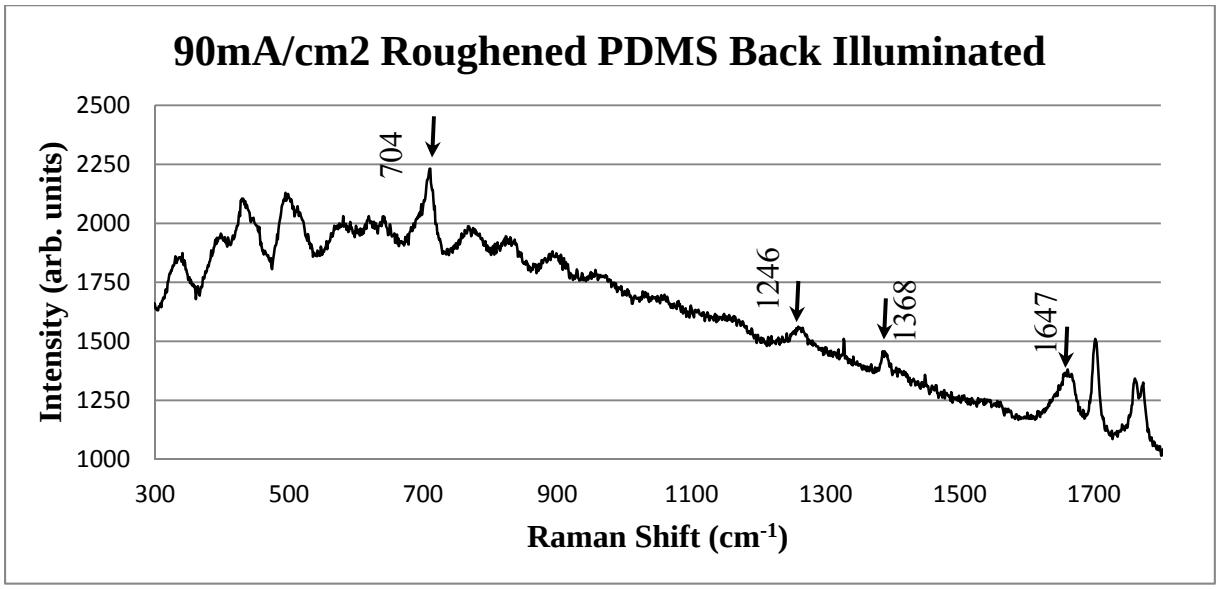

Figure 21: Back illuminated 90mA/cm^2 porous silicon pattern transferred onto PDMS, dipped in R6G.

3.3 Raman Spectra for 90mA/cm^2 SERS Substrates

A ~20 nm layer of Al was coated on roughened PDMS samples. In this case, these samples were obtained by transferring the nanostructures from the sample treated at 90mA/cm^2 for 35 minutes. Figure 22 shows the Raman spectra for front illuminated SERS substrate.

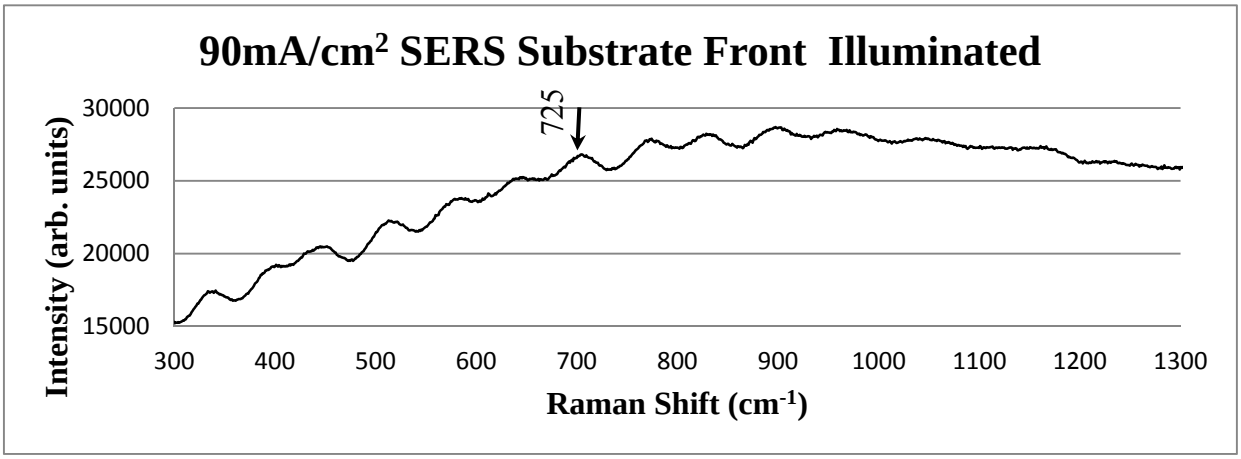

Figure 22 : 90 mA/cm^2 SERS substrate, R6G-coated, Al-coated, front illuminated.

Figure 23, on the other hand shows the Raman spectra for the same sample when back illuminated.

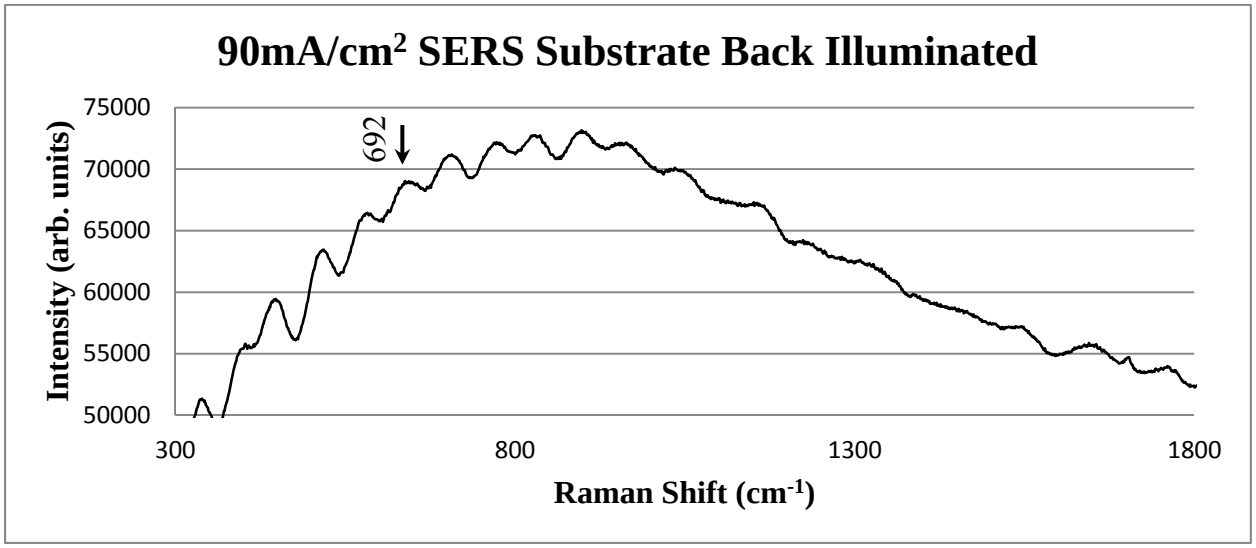

Figure 23: 90 mA/cm^2 SERS substrate, R6G-coated, Al-coated, back illuminated.

In both the cases, when focused, the spot size was larger than any of the previous samples. The lack in contrast in the peaks explains the major drawback of using the 10× objective lens.

3.4 Raman Spectra for 120 mA/cm^2 Reference Samples

Figure 24 shows the Raman spectra of a front illuminated roughened PDMS.

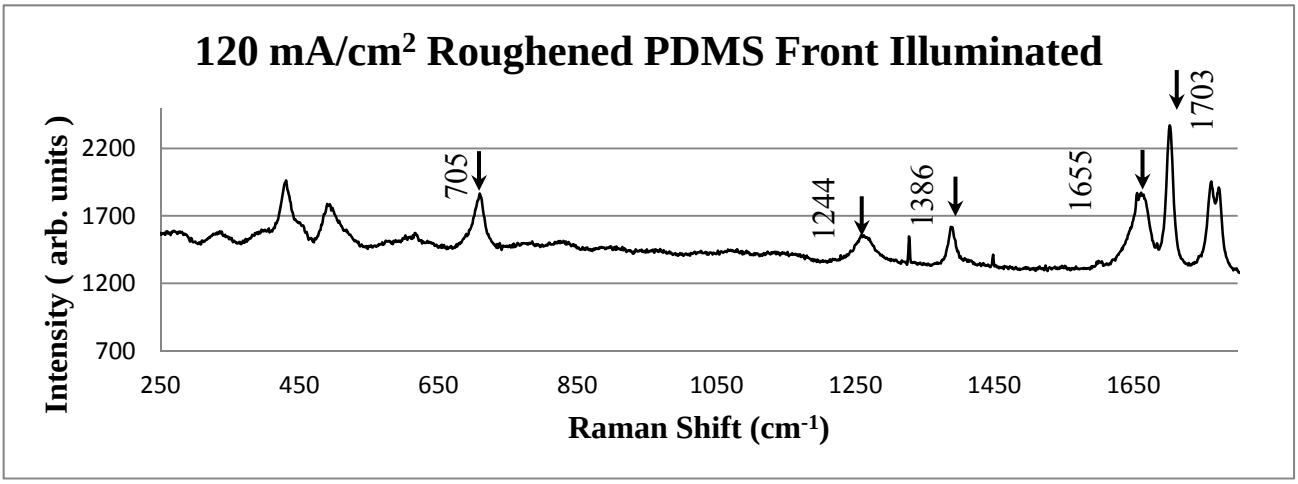

Figure 24 : Front illuminated 120 mA/cm^2 roughened PDMS sample, R6G-coated, Al-coated.

A thin layer of Al was sputtered on the porous silicon sample generated with an applied current density of 120 mA/cm^2. Figure 25 shows the Raman spectrum for this sample.

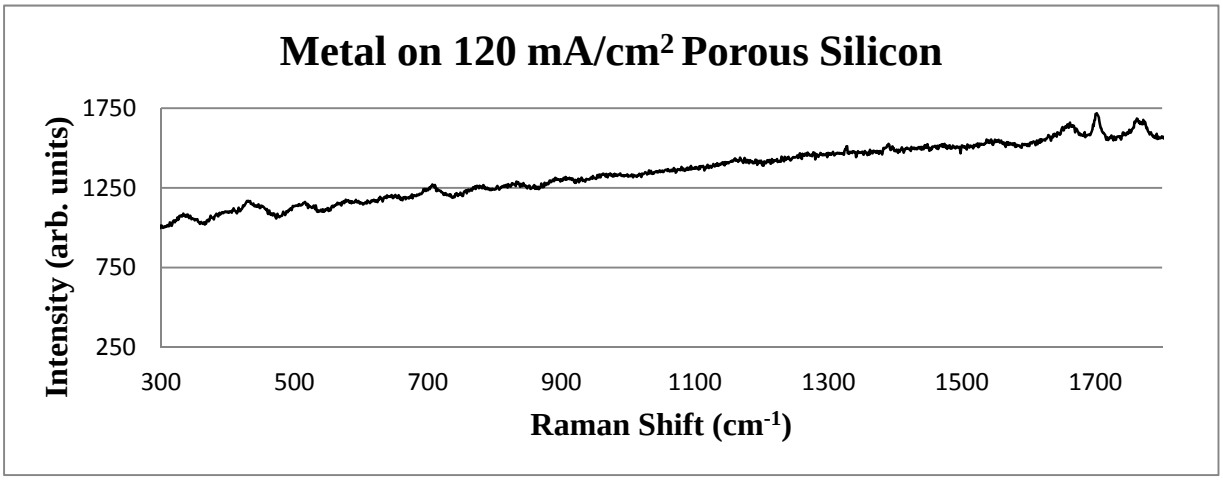

Figure 25 : 120 mA/cm^2 porous silicon coated with a thin layer of Al.

3.5 Raman Spectra for 120 mA/cm^2 SERS Substrates

The SERS substrate in Figure 26 was prepared by transferring the nanostructures from 120mA/cm^2 to a 10-to-1 PDMS and then coated with a thin layer of Al.

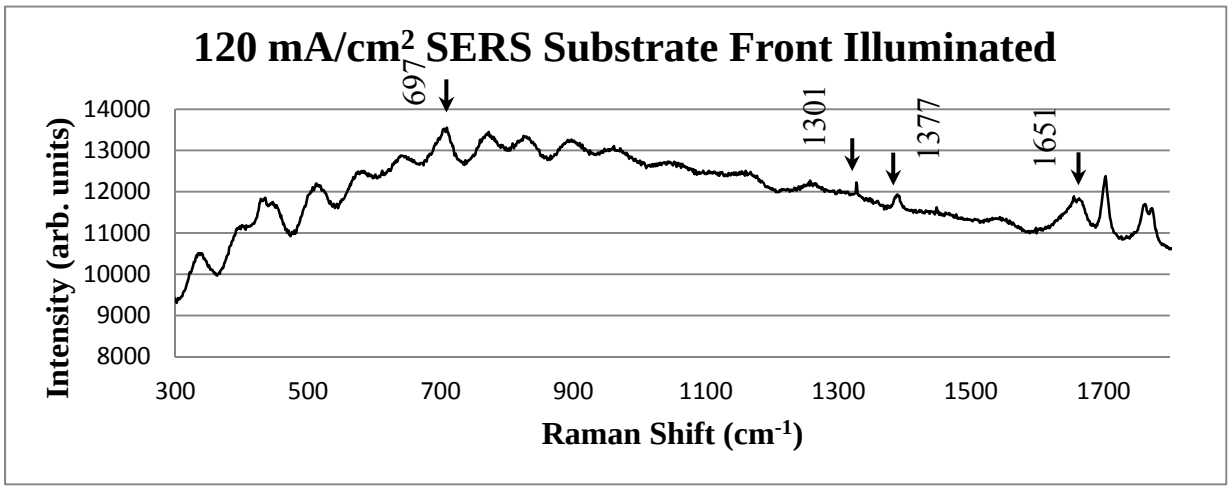

Figure 26 : Raman spectra of 120 mA/cm^2 porous silicon patterns transferred onto 10-to-1 PDMS, R6G-coated,Al-coated,front illuminated.

Before the Raman spectra were obtained, the sample was dipped in the analyte. Figure 26 shows the Raman spectra for this sample when front illuminated. The lack of the low contrast peaks is attributed to the larger spot size, when the sample is focused.

Figure 27 shows the Raman spectra for the 120 mA/cm^2 SERS substrate when back illuminated.

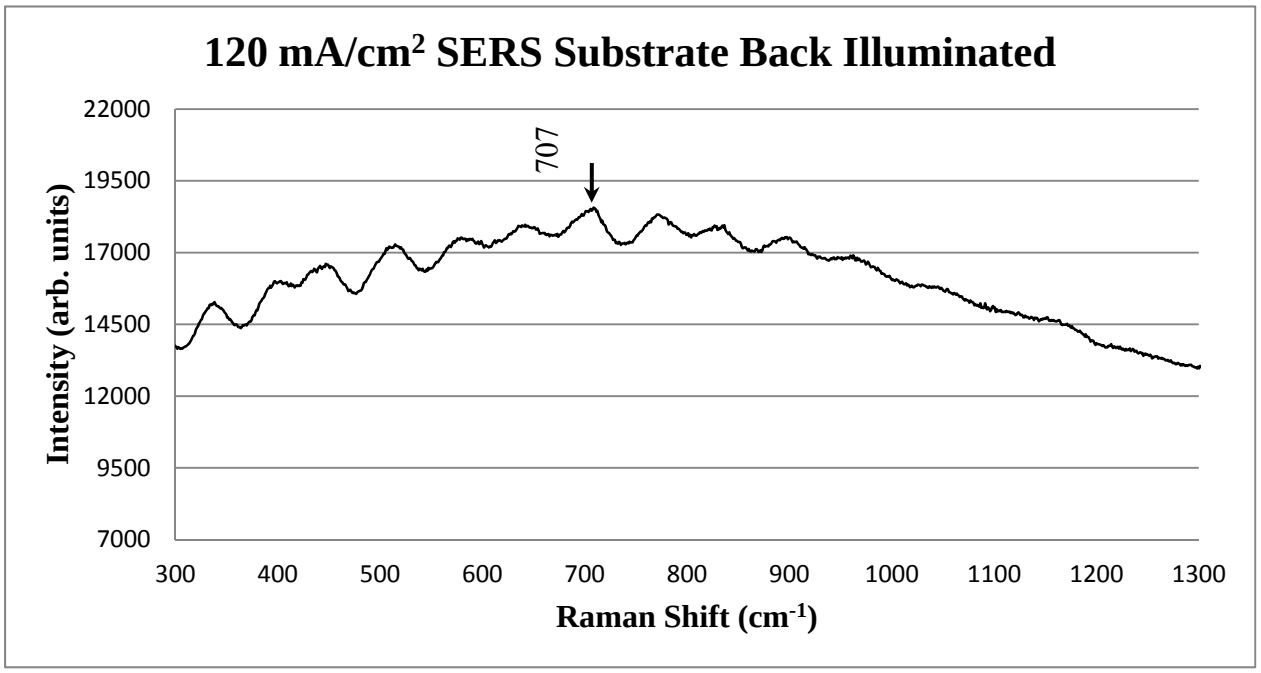

Figure 27: Raman spectra for 120mA/cm^2 SERS substrates,R6G-coated,Al-coated,back illuminated.

Chapter 4: Conclusion

It can now be conclusively said that the morphology of the underlying porous silicon layer is extremely critical for a successful SERS substrate. A uniform layer of porous silicon is equally important for the same. It was successfully achieved by depositing a 500nm layer of Al on the back side of the silicon wafer before commencing the etching process. The porous silicon layer generated was ~ 50nm deep and ~ 50 – 100 nm wide. Limiting the depth of the porous silicon layer helps reduce the strain on the PDMS sample during the "lift-off" process. Using a 10-to-1 PDMS instead of a less flexible 7-to-1 PDMS further assists the separation process. Using a mold release agent further reduces the complexity of the process.

It is expected that this technique is capable of producing effective SERS substrates. Improvements can be made to the Raman spectra by using a higher objective lens and low porosity underlying nanostructured porous silicon. Low porosity samples do not usually have structures as delicate as the high porosity samples thus helping the "lift-off" process.

Bibliography

1. University of Parma. Physics Department. Laboratory of Photoinduced Effects : Vibrational and X-Ray Spectroscopies. [Online] 2007. [Cited: October 1, 2011.] http://www.fis.unipr.it.

2. Berlin, Andrew. Nanotechnologies for ultra-sensitive molecular detection and manipulation. s.l. : Intel, 2004.

3. George C. Schats, Matthew A. Young, richard P. Van Duyne. Electromagnetic Mechanism of SERS. NorthWestern. [Online] 2006. [Cited: October 5, 2011.] http://chemgroups.northwestern.edu.

4. Raman spectra of pyridine adsorbed at a silver electrode. Fleischmann, M. 1974, Chemical Physics Letters.

5. Surface Raman Spectroelectrochemistry Part 1. Heterocyclic, Aromatic, and Aliphatic Amines Adsorbed on the Anodized Silver Electrode. Jeanmaire, David L and Van Duyne, Richard P. 1977, Journal of Electroanalytical Chemistry, pp. 16-18.

6. Dennis, Andrew. Surface Enhanced Raman Spectroscopy. PerkinElmer. [Online] 2007. [Cited: October 5, 2011.] http://www.perkinelmer.com.

7. Clearinghouse, Nanotech. Nano Letters. Nano Letters. DOI: 10.1021/nl200251a.

8. Single Molecule Detection Using Surface Enhanced Raman Scattering. Kneipp, Katrin. 1997, Physics Review Letters, pp. 1-4.

9. Kneipp, Katrin. Surface-enhanced Raman Scattering: Physics and Applications. Germany : Springer, 2006.

10. Surface-enhanced Raman Scattering: Imaging and Mapping of Langmuir Monolayers Physically Adsorbed onto Silver Island Films. Aroca, R.F. 12, Windsor : American Chemical Society, 1999, Vol. 16.

11. Kaiser Optical Systems, Inc. Raman Spectroscopy. Kaiser Optical Systems, Inc. [Online] Kaiser Optical Systems, Inc., 2011. [Cited: 10 2, 2011.] http://www.kosi.com/Raman_Spectroscopy.

12. Jiang, Shan. Term Paper for Physics 598 OS. Massachusetts Institue of Technology. [Online] [Cited: 10 1, 2011.] http://mit.edu/sjiang2/www/Resources/Term%20Paper_SERS.pdf.

13. www.dictionary.com. Colloid. Dictionary. [Online] [Cited: 10 12, 2011.] http://dictionary.reference.com/browse/Colloid?fromAsk=true&o=100074.

14. Adsorption and Surface-Enhanced Raman of Dyes on Silver and Gold Sols. Lee, P.C. and Meisel, D. 17, Argonne : Journal of Physical Chemistry, 1982, Vol. 86.

15. Ramos, Dr. Jose Vincente Garcia. Preparation and Analysis of Metal Colloids for SERS. www.pcoss.org. [Online] [Cited: 10 1, 2011.] www.pcoss.org.

16. A New Method for Fast Preparation of Highly Surface-Enhanced Raman Scattering (SERS) Active Silver Colloids at Room Temperature by Reduction of Silver Nitrate with Hydroxylamine Hydrochloride. Leopold, Nicolae and Lendl, Bernhard. 24, Vienna : Journal of Physical Chemistry, 2003, Vol. 107.

17. Assembly of Gold Nanostructured Films Templated by Colloidal Crystals and Use in Surface-Enhanced Raman Spectroscopy. Tessier, Peter M., et al., et al. 39, Newark : Journal of American Chemical Society, 2000, Vol. 122.

18. Colloid Filetration: A Novel Substrate Prepapration Method for Surface-Enhanced Raman Spectroscopy. Sutherland, William Scott and Winefordner, James D. 1, Gainesville : Journal of Colloid and Interface Science, 1992, Vol. 148.

19. SERS Substrates Fabricated by Island Lithography: The Silver/Pyridine System. Green, Mino and Liu, Feng Ming. London : American Chemical Society, 2003.

20. Multi-layer nanogap array for High-performance SERS substrate. Seol, Myeong-Lok, et al., et al. Daejeon : IOP Publishing, 2011.

21. Pu, Guang, et al., et al. Using PAA template to fabricate SERS substrate and the SERS detection of melamine. National Center for Biotechnology Information. [Online] [Cited: 10 1, 2011.] http://www.ncbi.nlm.nih.gov/sites/entrez?Db=pubmed&Cmd=Retrieve&list_uids=21137395&dopt=abstractplus. PMID:21137395 [PubMed - in process] .

22. Ling, K.J., et al., et al. Physica Status Solidi. Wiley Online Library. [Online] [Cited: 10 31, 2011.] http://onlinelibrary.wiley.com/doi/10.1002/pssa.2211280244/pdf.

23. Comparison of the Performance of SERS Substrates Fabricated by Deep UV Lithography and Nanosphere Lithography. Dinish, U. S., et al., et al. Singapore : AIP, 2010.

24. Schlegel, Vicki L. and Cotton, Therese M. Analytical Chemistry. ACS Publications. [Online] [Cited: 10 31, 2011.] http://pubs.acs.org/doi/abs/10.1021/ac00003a010.

25. Comparision of fibre-optic SERS sensors withe differently prepared tips. Viets, C. and Hill, W.

26. SERS-active substrates based on n-type porous silicon. Panarina, A. Yu., et al., et al. Minsk : Applied Surface Science, 2010, Vol. 256.

27. Preparation of SERS -Active Porous Gold Substrate. Ignat, Teodora, et al., et al. Bucharest : IEEE, 2004.

28. Abu-Hatab, Nahla A. Tennessee Research and Creative Exchange. The University of Tennessee Knoxville. [Online] May 2008. [Cited: 10 1, 2011.] http://trace.tennessee.edu/utk_graddiss/322/.

29. SERS-active Substrates Based on Metallic Nanocracks on PDMS. Mao, Haiyang, et al., et al. Nanocracks on PDMS : IEEE, 2011 .

30. Wikipedia. Porous Silicon. Wikipedia. [Online] [Cited: 10 1, 2011.] http://en.wikipedia.org/wiki/Porous_silicon#History.

31. Silicon Quantum wire Array Fabrication by Electrochemical and Chemical Dissolution of Wafers. Canham, L.T. 10, Worcestershire : Applied Physics Letters, 1990, Vol. 57. ISSN: 0003-6951.

32. Pérez, Elisabet Xifré. Design, Fabrication and Characterization of Porous SIlicon Multilayer Optical Devices. Tesis Doctorals en Xarxa. [Online] [Cited: 10 1, 2011.] http://tdx.cat/bitstream/handle/10803/8458/Cap2Fundamentals2.pdf?sequence=3. ISBN: 978-84-691-0362-3/DL: T.2181-2007.

33. George Green Institute of Electromagnetics Research. Porous Silicon. George Green Institute of Electromagnetics Research. [Online] [Cited: 10 1, 2011.] http://www.nottingham.ac.uk/ggiemr/downloads/hfa_chapter%202%20-%20Porous%20Silicon.pdf.

34. Porous silicon formation and electropolishing. Rauscher, Markus and Spohn, Herbert. 031604, New York : Physical Review E, 2001, Vol. 64.

35. Morphology and Formation Mechanisms of Porous Silicon. Zhang, X.G. Mississauga : Journal of Electrochemical Society, 2003, Vol. 151.

36. Efficient Raman Enhancement and Intermittent Light Emission Observed in Single Gold Nanocrystals. John T. Krug, II, et al., et al. 39, Bloomington : Journal of American Chemical Society, 1999, Vol. 121.

37. Direct Observation of Size-Dependent Optical Enhancement in Single Metal Nanoparticles. Emory, Steven R., Haskins, William E. and Nie, Shuming. 31, Bloomington : Journal of American Chemical Society, 1998, Vol. 120.

38. MEMC. High Resistivity Wafers. MEMC. [Online] [Cited: 10 1, 2011.] http://www.memc.com/assets/file/products/advanced-materials/hi-low%20res_rev10102003.pdf.

39. Princeton Instruments. Raman Spectroscopy Basics. Princeton Instruments. [Online] [Cited: 10 1, 2011.] http://content.piacton.com/Uploads/Princeton/Documents/Library/UpdatedLibrary/Raman_Spectroscopy_Basics.pdf.

40. Whitney, Alyson V., Duyne, Richard P. Van and Casadio, Francesca. Silver Island Films as Substrate for Surface-enhanced Raman Spectroscopy (SERS): A Methodological Study on Their Application to Artists' Red Dyestuffs. The Van Duyne Group. [Online] [Cited: 7 11, 2011.] http://chemgroups.northwestern.edu/vanduyne/pdf/sers_reddye_SPIE_2006.pdf.

41. Chemical Imaging in a Surface Forces Apparatus: Confocal Raman Spectroscopy of Confined Poly(dimethylsiloxane). Bae, Sung Chul, et al., et al. Urbana : Langmuir, 2005.

42. DFT Vibrational Calculations of Rhodamine 6G Adsorbed on Silver: Analysis of Tip-Enhanced Raman Spectroscopy. Watanabe, Hiroyuki, et al., et al. 11, Wako : Journal of Physical Chemistry, 2005, Vol. 109.

43. Wikipedia. Surface Enhanced Raman Spectroscopy. Wikipedia. [Online] [Cited: October 1, 2011.] http://www.wikipedia.org.

44. Anomalously Intense Raman Spectra of Pyridine at a Silver Electrode. Albrecht, Grant M and Creighton, Alan J. 1977, Journal of American Chemical Society.

45. SERRS of Langmuir-Blodgett Monolayers: Spatial Spectroscopic Tuning. Aroca, Ricardo. 1989, Journal of American Chemical Society, pp. 1-3.

46. Nanowell Surface Enhanced Raman Scattering Arrays Fabricated by Soft- Lithograohy for Label-free Biomolecular Detections in Integrated Microfluidics. Lee, Luke P. and Liu, Gang L. Berkeley : Applied Physics Letters, 2005, Vol. 87. DOI: 10.1063/1.2031935.

47. The Optical Constants of Silver, Gold,Copper and Aluminum. L.G.Schulz. 5, Chicago : Journal of Optical Society of America, 1953, Vol. 44.

48. Surface-Enhanced Resonance Raman Spectroscopy of Rhodamine 6G Adsorbed on Colloidal Silver. Hildebrandt, Peter and Stockburger, Manfred. 24, Gottingen-Nikolausberg : Journal of Physical Chemistry, 1984, Vol. 88.

Vita

Pallavi Rao Malempati was born and brought up in the Orange capital of India- Nagpur, Maharashtra. Her parents inspired her to pursue a bachelor's degree in electronics engineering from one of the premier institutes in Maharashtra. Armed with a bachelor's degree in electronics engineering and the will to learn more, Pallavi joined Louisiana State University in Baton Rouge, Louisiana.